PERGAMON

International Journal of Solids and Structures 38 (2001) 5215–5222

INTERNATIONAL JOURNAL OF SOLIDS and STRUCTURES

www.elsevier.com/locate/ijsolstr

The application of B–P constitutive equations in finite element analysis of high velocity impact

Shun-Cheng Song [a,*], Zhu-Ping Duan [b], Duo-Wang Tan [c]

[a] *Department of Applied Mechanics, Southwest Jiao Tong University, Chengdu 610031, People's Republic of China*
[b] *Institute of Mechanics, Chinese Academy of Sciences, Beijing 100080, People's Republic of China*
[c] *Southwest Institute of Fluid Physics, CAEP, Mianyang 621900, People's Republic of China*

Received 14 February 2000; in revised form 26 May 2000

Abstract

We present in this paper the application of B–P constitutive equations in finite element analysis of high velocity impact. The impact process carries out in so quick time that the heat-conducting can be neglected and meanwhile, the functions of temperature in equations need to be replaced by functions of plastic work. The material constants in the revised equations can be determined by comparison of the one-dimensional calculations with the experiments of Hopkinson bar. It can be seen from the comparison of the calculation with the experiment of a tungsten alloy projectile impacting a three-layer plate that the B–P constitutive equations in that the functions of temperature were replaced by the functions of plastic work can be used to analysis of high velocity impact. © 2001 Published by Elsevier Science Ltd.

Keywords: Constitutive equation; High velocity impact; Finite element analysis

1. Introduction

In recent years, more realistic constitutive equations have been proposed for the combined elastic and time-dependent inelastic deformation of metals. One class of such equations is referred to as "unified" in the sense that all inelastic deformations are represented by the same variables. These equations also include load history-dependent variables to represent certain aspects of the material state, e.g. hardening and softening. Some of the proposed sets of "unified" constitutive equations do not require a prescribed yield criterion and loading/unloading conditions. The B–P constitutive equations proposed by Bodner and Partom (1975) for elastic–viscoplastic response are of this class and have been adopted in the finite element calculations of high velocity impact in this paper. For the convenience of calculations the heat conducting in the impact process was neglected and some parameters versus temperature were superseded by the functions of plastic work. The material constants in the equations have been determined by comparison of the one-dimensional calculations with the experiments of Hopkinson bar.

* Corresponding author.

0020-7683/01/$ - see front matter © 2001 Published by Elsevier Science Ltd.
PII: S0020-7683(00)00328-0

2. Bodner–Partom equations and its applications

In the Bodner–Partom constitutive equations the total strain rate tensor is considered to be composed of an elastic part, $\dot{\varepsilon}^{e}_{ij}$ and an inelastic (plastic) part, $\dot{\varepsilon}^{p}_{ij}$ at all stages:

$$\dot{\varepsilon}_{ij} = \dot{\varepsilon}^{e}_{ij} + \dot{\varepsilon}^{p}_{ij} \tag{2.1}$$

According to the Hooke's law, the stress tensor reads:

$$\dot{\sigma}_{ij} = \lambda \dot{\varepsilon}^{e}_{kk}\delta_{ij} + 2G\dot{\varepsilon}^{e}_{ij} \tag{2.2}$$

where λ and G are Lame coefficients and δ_{ij} is the Kronecker delta symbol tensor.

From the Bodner–Partom law, the second invariant of the plastic strain rate tensor can be given by:

$$D^{p}_{2} = D^{2}_{0}\exp\left[-\left(\frac{Z^{2}}{3J_{2}}\right)^{n}\right] \tag{2.3}$$

$$D^{p}_{2} = \frac{1}{2}\dot{\varepsilon}^{p}_{ij}\dot{\varepsilon}^{p}_{ij} \tag{2.4}$$

$$J_{2} = \frac{1}{2}S_{ij}S_{ij} \tag{2.5}$$

$$S_{ij} = \sigma_{ij} - \frac{1}{3}\sigma_{kk}\delta_{ij} \tag{2.6}$$

$$Z = Z_{1} + (Z_{0} - Z_{1})\exp(-mw^{p}/Z_{0}) \tag{2.7}$$

$$\dot{w}^{p} = \sigma_{ij}\dot{\varepsilon}^{p}_{ij} \tag{2.8}$$

where Z_0, Z_1 and m are material constants. The parameter D_0 corresponds to the limiting strain rate and this interpretation is inherent in the functional form of Eq. (2.3). The material parameter n controls strain rate sensitivity and the overall level of the flow stress.

From the plastic flow law and Eq. (2.3), the plastic strain rate tensor can be given by:

$$\dot{\varepsilon}^{p}_{ij} = (D^{p}_{2}/J_{2})^{1/2}S_{ij} \tag{2.9}$$

The Eqs. (2.1)–(2.9) can be directly introduced into the finite element code for analysis of high velocity impact, in which the calculations and integration are performed on an element-by-element and a step-by-step basis. For each new step the strain rate tensor, $\dot{\varepsilon}_{ij}$ in Eq. (2.1) can be obtained from geometrical relations but the values of the plastic part, $\dot{\varepsilon}^{p}_{ij}$ at advanced time step must be taken to determine the elastic part $\dot{\varepsilon}^{e}_{ij}$. Then, the stress rate tensor, $\dot{\sigma}_{ij}$ can be given from Eq. (2.2) and the stress tensor can be obtained by integration:

$$\sigma_{ij} = S_{ij} - (P + Q)\delta_{ij} + \dot{\sigma}_{ij}\,\Delta t \tag{2.10}$$

where the deviatoric stress tensor S_{ij}, the hydrostatic pressure P and the artificial viscosity Q take the values of that at advanced step. The artificial viscosity tends to eliminate spurious oscillations which would otherwise occur for wave propagation problems. This technique was originally proposed by von Neumann and Richtmyer (1950). It is expressed in terms of linear and quadratic components and is applied only when the volumetric strain rate $\dot{\varepsilon}_{V}$ is negative:

$$\begin{aligned} &Q = C_{l}\rho C_{s}h|\dot{\varepsilon}_{V}| + C^{2}_{0}\rho h^{2}(\dot{\varepsilon}_{V})^{2} && \text{for } \dot{\varepsilon}_{V} < 0 \\ &Q = 0 && \text{for } \dot{\varepsilon}_{V} \geqslant 0 \end{aligned} \tag{2.11}$$

where C_s and ρ are the sound velocity and the density of the material respectively and h is the minimum altitude of the element. Typical values used for the dimensionless coefficients are $C_l = 0.5$ and $C_0^2 = 4.0$ (see e.g. Wilkins (1964)). The hydrostatic pressure is dependent on the volumetric strain and the internal energy in the element. From the complete expression of the Mie–Gruneisen equation it is given by (see e.g. Walsh et al. (1957)):

$$P = (k_1\mu + k_2\mu^2 + k_3\mu^3)\left(1 - \frac{\Gamma\mu}{2}\right) + \Gamma E_s(1+\mu) \tag{2.12}$$

where $\mu = (V_0/V) - 1$, k_1, k_2 and k_3 are material-dependent constants and Γ is the Gruneisen coefficient. The specific internal energy, E_s is obtained from the plastic work done on the element by the various stresses.

The plastic strain rate tensor, $\dot{\varepsilon}_{ij}^{p}$ for new step can be obtained by Eqs. (2.3)–(2.9) after the stress tensor is given by Eq. (2.10).

3. Dimensionless material constants and high velocity impact

The material constants Z_0, Z_1 and m in the Bodner–Partom constitutive equations could become dimensionless, and the composition of m/Z_0 in Eq. (2.7) could be replaced by m, if the stress tensor σ_{ij} is normalized by the static yield stress σ_0.

In Eq. (2.3) the material parameter n which controls strain rate sensitivity and the overall level of the flow stress depends on the transient temperature.

According to Batra and Kim (1990) the dimensionless n can be expressed as that $n = (\theta_{melt}/\theta) + b$, where θ_{melt} and θ are melting temperature and transient temperature of material respectively and b is a dimensionless constant. Since the material parameter n is a function of transient temperature, for each step of finite element analysis the heat-conducting calculations which are much costly must be performed. In fact, the process of the high velocity impact is performed in so quick time that the heat-conducting takes hardly place, so the process of the high velocity impact can be approximately considered as a no heat-conducting process for which the heat-conducting calculations can be neglected. Consequently, the dimensionless material parameter n can be expressed as a function of plastic work, i.e. $n = n_a E_a/(w^p + E_a) + b$, where E_a is the initial specific internal energy of material, which depends on the ambient temperature of the material and w^p is the plastic work done on the element by the various stresses and the dimensionless constant $n_a = \theta_{melt}/\theta_a$, where θ_a represents the ambient temperature of the material.

It is noted that the shear modulus G in Eq. (2.2) varies with the temperature of the material. Batra and Kim (1990) have given the modulus G of carbon steel versus temperature θ shown in Fig. 1, where G and θ

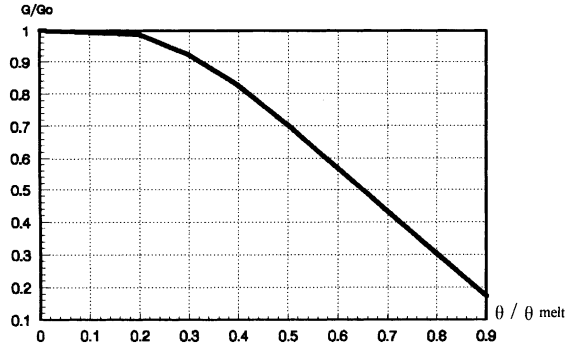

Fig. 1. Shear modulus G versus θ.

are normalized by the modulus G_0 measured at room temperature and by the melting temperature θ_{melt} respectively. In fact this relation of G/G_0 to $\theta/\theta_{\text{melt}}$ is approximately found for many metals and has been used for armor steel, tungsten alloy and aluminium alloy in this paper. Because the heat-conducting calculations have been neglected as indicated above, the dimensionless variable $\theta/\theta_{\text{melt}}$ is superseded in this paper by the dimensionless variable of plastic work $(w^{\text{p}} + E_{\text{a}})/(n_{\text{a}}E_{\text{a}})$.

4. Determination of dimensionless material constants

In order to determine the dimensionless material constants Z_0, Z_1 and m in the Bodner–Partom constitute equations, the experimental strain–stress data of the material at various strain rate need first to be measured. Then the values of these parameters can be sought by making comparison between calculated results and experimental data.

The Hopkinson (or Kolsky) bar that has found a wide acceptance as the instrument for intermediate strain testing (10^2–10^4 s^{-1}) was used in this paper to measure the strain–stress data of materials. Here a small cylindrical specimen was sandwiched between two long loading bars. Strain gauges on the input bar recorded the incoming impact wave $\varepsilon_{\text{I}}(t)$ and the returning reflected wave $\varepsilon_{\text{R}}(t)$ from the specimen while strain gauges on the output bar recorded stress wave $\varepsilon_{\text{T}}(t)$ transmitted through the specimen. From these three elastic signal the dynamic stress–strain data for the specimen might be derived (see e.g. Kolsky (1949)):

$$\sigma(t) = E_0 \frac{A_0}{A} \varepsilon_{\text{T}}(t) \tag{4.1}$$

$$\varepsilon(t) = \frac{C_0}{L} \int_0^t [\varepsilon_{\text{I}}(t) - \varepsilon_{\text{R}}(t) - \varepsilon_{\text{T}}(t)]\,\mathrm{d}t \tag{4.2}$$

where E_0, C_0 and A_0 represent the elastic modulus, sound velocity and cross-sectional area of the bar respectively and A and L represent the cross-sectional area and length of the specimen respectively. It should be noted that in order to smooth the strain–stress data that were always oscillatory more or less, in our paper the average value of 4 nearby points has been taken as the value of each point.

For advanced given constants of the material and the boundary conditions in the Hopkinson bar experiment, the strain–stress relationship can also be obtained by the one-dimensional numerical calculations, in which the control equations with inclusion of the one-dimensional Bodner–Partom equations read:

$$v_{x1} = v_0, \quad v_{x2} = 0 \tag{4.3}$$

$$\dot{\varepsilon}_x = \frac{\partial v_x}{\partial x} = \dot{\varepsilon}_x^{\text{e}} + \dot{\varepsilon}_x^{\text{p}} \tag{4.4}$$

$$\dot{\sigma}_x = 2(1+v)G(w^{\text{p}})\dot{\varepsilon}_x^{\text{e}} \tag{4.5}$$

$$\dot{\varepsilon}_x^{\text{p}} = \frac{2D_0}{\sqrt{3}} \frac{\sigma_x}{|\sigma_x|} \exp[-0.5(3Z^2/\sigma_x^2)^n] \tag{4.6}$$

$$n = \frac{n_{\text{a}}E_{\text{a}}}{w^{\text{p}} + E_{\text{a}}} + b, \quad b = 0 \tag{4.7}$$

$$Z = Z_1 + (Z_0 - Z_1)\exp(mw^{\text{p}}), \quad \dot{w}^{\text{p}} = \sigma_x \dot{\varepsilon}_x^{\text{p}} \tag{4.8}$$

where v_x represents the axial displacement velocity, but v_{x1} and v_{x2} represent the displacement velocity on each contact surface respectively and the other symbols is as mentioned above. The numerical calculations

can be started from Eq. (4.3) and the strain rate $\dot{\varepsilon}_x$ can be calculated from geometrical Eq. (4.4) and the elastic strain rate $\dot{\varepsilon}_x^{\mathrm{e}}$ can be obtained by taking the plastic part, $\dot{\varepsilon}_x^{\mathrm{p}}$ at advanced time. Consequently, the stress σ_x can be calculated by integrating Eq. (4.5), in which the value of the plastic work w^{p} at advanced time is also taken and then the plastic strain rate $\dot{\varepsilon}_x^{\mathrm{p}}$ at this stage of the deformation process can be obtained from Eq. (4.6).

Through cycling calculations the material stress–strain relationship can be obtained, but in general the first calculations could not bear comparison with the experimental results and the material constants Z_0, Z_1 and m need to be adjusted and the calculations need to be renewed until the calculated stress–strain curves close to the experimental curves at various strain rate.

In this paper two sets of experiments for armor steel, tungsten alloy and aluminium alloy were performed to determine their constants Z_0, Z_1 and m respectively in the Bodner–Partom constitutive equations. One set of experiments was performed with lower strain rate and another set with higher strain rate. By repeated comparison of the numerical calculations with the results of Hopkinson bar experiment, the dimensionless constants Z_0, Z_1 and m for armor steel, tungsten alloy and aluminium alloy have been determined respectively and are shown in Table 1, where $D_0^{(1)}$ and $D_0^{(2)}$ are corresponding to lower strain rate and higher strain rate respectively. It should be noted that $D_0^{(1)}$ and $D_0^{(2)}$ are large compared with experimental strain rate.

Table 2 illustrates the material static mechanical parameters at room temperature, that have been used for calculations. Figs. 2–4 show the plots of the axial compressive stress versus strain for armor steel, tungsten alloy and aluminium alloy respectively. It can be seen from Figs. 2–4 that the result of calculations using the material constants in Table 1 is in good agreement with the corresponding result of experiments.

5. Calculation example

The high velocity impact problem that a tungsten alloy projectile penetrates into a three-layer plate at initial velocity 1560 m s^{-1} was solved by incorporating the unified elastic–viscoplastic constitutive equations of Bodner–Partom into the finite element code. The length of the projectile was 93 mm and its radius was 3 mm. The first and the third layer of the plate were armor steel which thickness were 21 and 50 mm respectively, and the second layer of the plate was aluminium alloy which thickness was 26 mm. The material constants Z_0, Z_1 and m used in constitutive equations were chosen as shown in Table 1 and the other static mechanical parameters were as shown in Table 2.

Table 1
The constants and D_0 for armor steel, tungsten alloy and aluminium alloy

Material	$D_0^{(1)}$ (s^{-1})	$D_0^{(2)}$ (s^{-1})	Z_0	Z_1	m
Armor steel	2.5×10^3	5.0×10^3	0.81	1.08	8.5
Tungsten alloy	1.5×10^3	4.5×10^3	0.78	1.12	8.5
Aluminium alloy	6.8×10^2	2.5×10^3	0.75	1.28	1.5

Table 2
The static mechanical parameters of material at room temperature

Material	ρ (kg m^{-3})	G_0 (MPa)	v	σ_0 (MPa)	E_{a} (J m^{-3})
Armor steel	7.8×10^3	7.7×10^4	0.3	9.5×10^2	8.24×10^8
Tungsten alloy	17.8×10^3	1.5×10^5	0.2	8.5×10^2	6.04×10^8
Aluminium alloy	2.7×10^3	2.71×10^4	0.33	4.3×10^2	4.20×10^8

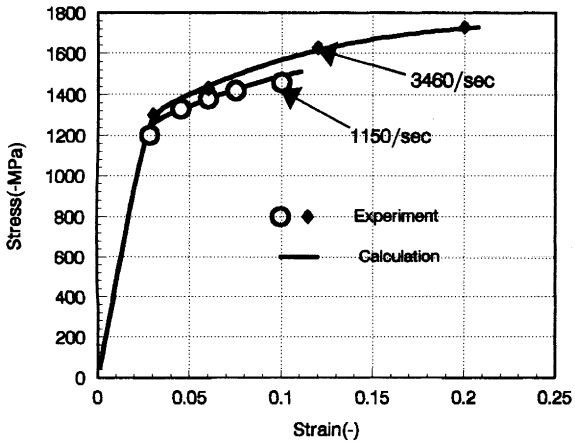

Fig. 2. Plots of stress versus strain for armor steel.

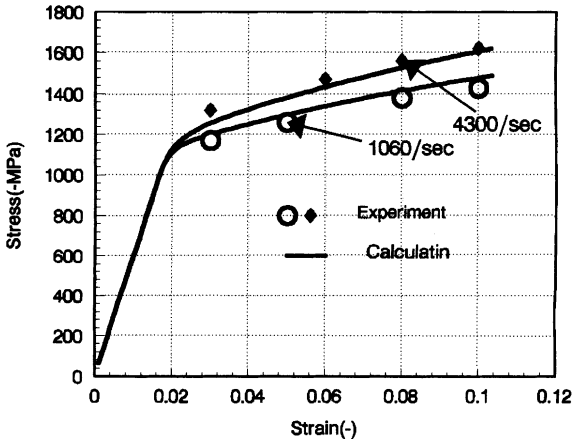

Fig. 3. Plots of stress versus strain for tungsten alloy.

It is necessary to note that the actual strain rate in the penetrating process is hardly measured, therefore the parameter D_0 in the constitutive equations was chosen only by trial calculations. In this paper the trial calculations were performed in the assessed range of $10^5\ s^{-1}$ according to Zukas et al. (1982), Swegle and Grady (1985), Anderson and Walker (1991) and the parameter D_0 for each material was chosen as shown in Table 3.

In this computations the eroding interface algorithm proposed by Johnson and Stryk (1987) has been used and the tungsten alloy element was assumed to fail completely when its equivalent plastic strain arrived at 0.12, but the armor steel and the aluminium alloy element was assumed to fail at 0.28 and 0.21 respectively, where the failure criterion was slightly larger than the material elongation.

As the computational results, when the momentum of the projectile reduced to zero its penetrating depth and its residual length were 84 and 18 mm respectively which were in good agreement with that of the experiment. The final profiles of the calculation and the experiment are shown in Figs. 5 and 6 respectively.

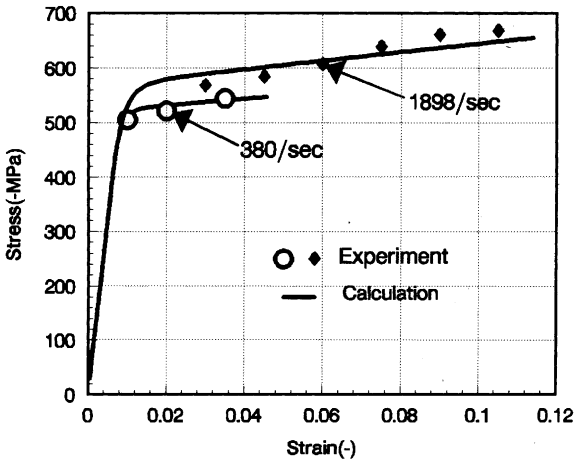

Fig. 4. Plots of stress versus strain for aluminium alloy.

Table 3
The parameter D_0 for each material

Material	D_0 (s^{-1})
Armor steel	6.80×10^5
Tungsten alloy	6.20×10^5
Aluminium alloy	6.50×10^5

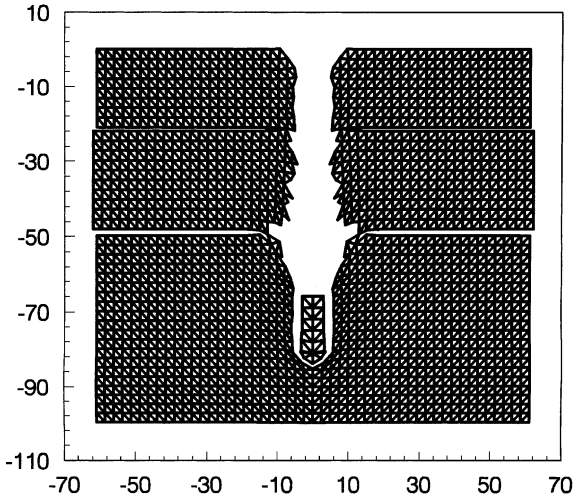

Fig. 5. The result of the calculation.

6. Conclusions

The Bodner–Partom elastic-viscoplastic constitutive equations could been applied to finite element calculations of high velocity impact. The impact process can be approximately considered as a no

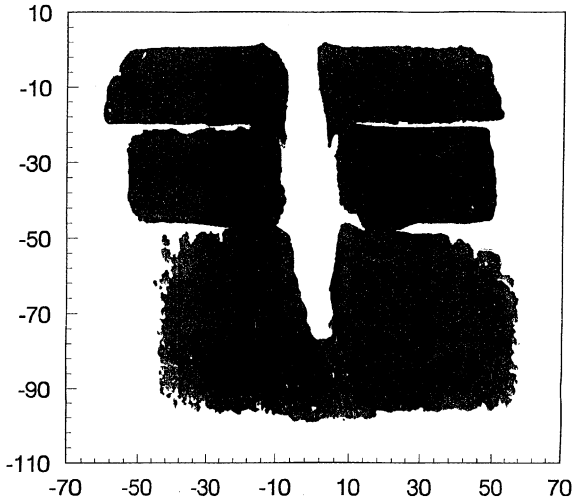

Fig. 6. The result of the experiment.

heat-conducting process and the parameter n and G in the equations are thence considered as the function of plastic work rather than the function of temperature. The dimensionless constants Z_0, Z_1 and m of material in the equations can be determined by comparison of the one-dimensional calculations with the experiments of Hopkinson bar, but the determination of parameter D_0 needs making trial calculations. In this paper, the result of calculation that a tungsten alloy projectile penetrates a three layer plate is in good agreement with the result of corresponding experiment.

Acknowledgements

The authors acknowledge the financial support (No.19772042) from the Natural Science Foundation and (No.98010102) from the AEP Science Foundation of China.

References

Anderson Jr., C.E., Walker, J.D., 1991. An examination of long-rod penetration. Int. J. Impact Engng. 11, 481–501.

Batra, R.C., Kim, C.H., 1990. Effect of viscoplastic flow rules on the initiation and growth of shear bands at high strain rates. J. Mech. Phys. Solids 38, 859–874.

Bodner, S.R., Partom, Y., 1975. Constitutive equations for elastic–viscoplastic strain-hardening materials. J. Appl. Mech. 42, 385–389.

Johnson, G.R., Stryk, R.A., 1987. Eroding interface and improved tetrahedral element algorithms for high-velocity impact computations in three dimensions. Int. J. Impact Engng. 5, 411–421.

Kolsky, H., 1949. An investigation of mechanical properties of materials at very high rates of loading. Proc. Phys. Soc. (Lond.) B 62, 676–700.

Swegle, J.W., Grady, D.E., 1985. J. Appl. Phys. 58, 692.

Walsh, J.M., et al., 1957. Shock wave compressions of twenty-seven metals: equations of state of metals. Phys. Rev. 108, 196–296.

Wilkins, M.L., Calculation of elastic–plastic flow. In: Alder, B., Fernback, S., Rottenberg, M. (Eds.), Methods in Computational Physics, vol. 3. Academic Press, New York, 1964.

von Neumann, J., Richtmyer, R.D., 1950. A method for numerical calculation of hydrodynamic shocks. J. Appl. Phys. 21, 232–237.

Zukas, A. Impact Dynamics. Wiley, New York, 1982.